

Simultaneous thermodynamic and transport measurements of the field-induced spin-density-wave transitions in $(\text{TMTSF})_2\text{ClO}_4$

U.M. Scheven, E.I. Chashechkina, E. Lee, and P.M. Chaikin

Department of Physics, Princeton University, Princeton, New Jersey 08544

(Received 23 December 1994)

The standard model for the field-induced spin-density-wave (FISDW) transitions in the Bechgaard salts $(\text{TMTSF})_2X$, where TMTSF is tetramethyltetraselenafulvalene, explains a cascade of phase transitions with each phase associated with the quantum Hall effect. The ClO_4 salt is sufficiently different that it has inspired a series of theoretical modifications from the standard model. To test these models we have performed simultaneous ρ_{xx} , ρ_{xy} , specific-heat, magnetocaloric effect, and magnetization measurements in the field range from 0–9 T. We find that all of the transport transitions, specifically the Hall resistance jumps, are associated with thermodynamic transitions. We observe the emergence of a new FISDW state characterized by a distinct Hall plateau. It arises from what was originally believed to be a tetracritical point in the phase diagram. We find no evidence for an arborescent phase diagram, but rather the signature of a single pairwise splitting of the phase boundaries. The higher-field transitions are decidedly first order, hysteretic, and “lossy.” Anion disorder decreases the number of observed phases and shifts the transition fields.

I. INTRODUCTION

The quasi-one-dimensional organic conductors $(\text{TMTSF})_2X$, where TMTSF is tetramethyltetraselenafulvalene, display a variety of unusual properties. Among these are superconductivity, field-induced spin-density waves, SdH-like oscillations of the magnetoresistance, quantized Hall resistance reminiscent of the quantum Hall effect (QHE), and metallic reentrance at high fields.¹ The abundance of magnetic-field-dependent phenomena is most striking because the Fermi surface of these materials consists of two disconnected warped sheets, and there are no closed orbits in the absence of a magnetic field. The formation of a field-induced spin-density wave is understood in terms of the “standard model,” and variations thereof, as proposed by Gor’kov and Lebed.² In the standard model the two sheets of the Fermi surface are imperfectly nested by a spin-density wave (SDW) wave vector \mathbf{Q} , giving rise to small carrier pockets and closed orbits. In the presence of a magnetic field there is Landau quantization and the energy is lowered whenever the Fermi level sits between Landau levels. This occurs when the area of the small pockets is an integer n_A times the quantized area $eH/\hbar c$. As the magnetic field is increased the wave vector \mathbf{Q} changes continuously in such way as to keep the quantized area. At certain fields it changes discontinuously to allow a different integer. The result is a cascade of transitions with different \mathbf{Q} vectors, each associated with a quantized hall resistance $\rho_{xy} = h/Ne^2$. In the standard model the transitions between field-induced spin-density-wave (FISDW) states are first-order transitions associated with changes of Q_x , the x component of the spin-density wave vector \mathbf{Q} , by one magnetic wave vector $\delta = ebH/\hbar c$. Phases where $Q_x = 2k_f + n\delta$ are then labeled by the (integer) quantum number n . In the simplest case the integers n_A , N , and n are equal. The

initial transition from the metallic state to the FISDW state is a second-order transition.

The standard model explains the basic phenomena and semiquantitatively “works” for $(\text{TMTSF})_2\text{PF}_6$ under pressure. However, the ClO_4 salt, which undergoes these transitions at ambient pressure, and is therefore much more widely studied, has shown qualitative disagreement with the simple form of the standard model.³ In particular, there are unexpected sign reversals in the Hall coefficient,⁴ reentrance of the metallic phase at both high and low field, and reports of a complex, branched, tree-like or arborescent phase diagram at low temperature.⁵ The standard model has been modified by several groups to account for these deviations. There are two main points addressed in the modifications, the fact that in all the Bechgaard salts the chains are dimerized in the most conducting \mathbf{a} direction and the fact that, for the ClO_4 salt there is an anion ordering transition at 24 K which doubles the unit cell in the \mathbf{b} direction. The dimerization along \mathbf{a} means that electron-electron Umklapp scattering and commensurability may be important since $4k_F = 2\pi/a$. The anion ordering can create two inequivalent chains and two separate bands with two Fermi surfaces.

In the “standard model” and its modifications there are many questions relating to the coexistence or competition of the spin-density-wave phases with different quantum numbers “ n ” as well a suggestion that we may have different transitions for the thermodynamic quantities and the transport quantities. In particular the Hall quantum number N may not simply be related to n or n_A especially if spin-density waves exist with many density-wave components of different n . Multiple order-parameter scenarios have been proposed^{6,7} to explain several reported experimental phenomena including a tetracritical point and the “arborescent” phase boundary.⁵

The experiments described below were conducted to address a number of these issues. There is the question as to whether or not the phase diagram is arborescent. In earlier work, down to 0.5 K, we found no evidence for arborescence, but evidence of a tetracritical point in the phase diagram and a single splitting of many of the FISDW transition lines.⁸ These measurements are here extended to 0.3 K. However, the main contribution of this paper is the simultaneous measurement of several transport and thermodynamic properties on the same sample, as temperature and field are varied. We can then reliably correlate the thermodynamic and transport properties, a correlation which thus far has been elusive because experimental results strongly depend on the degree to which the anions have ordered, and because in many cases the slight misorientation of the c^* axis of the sample with the applied field makes comparison between different experiments unreliable. Among other things, this experimental difficulty has thus far made it impossible to answer the question whether or not there are indeed changes of ρ_{xy} within a given FISDW phase, or even thermodynamic transitions which do not appreciably affect the transport properties. The present simultaneous thermodynamic and transport measurements enable us to correlate well these signatures of the FISDW transitions. We address the question of whether the transitions between FISDW states are first or second order. We also present data on the temperature dependence and value of ρ_{xy} , and present attempts to find the “fast oscillations”⁹ observed in resistance in thermodynamic measurements in the metallic state.

Our main findings include the absence of “arborescence” in the low-temperature phase diagram, but the presence of a single splitting in the boundary between two SDW phases. We find a complete overlap of each thermodynamic transition with each transport transition. In a separate matter the temperature dependence of ρ_{xy} indicates Hall plateau ratios of 1:3:5 in partial support of a recent model by Osada, Kagoshima, and Miura.¹⁰ A simple phenomenological Landau treatment suggests that the phase boundary splitting results from a temperature-dependent repulsion between phases with different n . However, the “tetracritical point” previously reported has an unexpected ρ_{xy} behavior inconsistent with a simple Landau picture.

II. EXPERIMENTAL METHODS

Ideally we would have liked to perform all experiments on the same sample. However, specific heat and magnetization have some conflicting requirements. As the next best thing, experiments were conducted with two samples of $(\text{TMTSF})_2\text{ClO}_4$ mounted on the same He^3 cryostat so that they would experience identical slow cooling (8.9 mK/min) through the anion ordering transition, yielding very relaxed samples.

On one sample we measured heat capacity, magnetocaloric effect, Hall and magnetoresistance. The 1.9 mg sample of ClO_4 salt was suspended in vacuum from six low thermal conductivity wires that were attached to the

sample with silver paint. These wires were used to measure ρ_{xx} and ρ_{xy} . The sample was oriented with $c^* // H$. A low mass thick-film thermometer and a small heater were attached to the sample with Apiezon *N* grease. The wires to these elements were also made of low thermal conductivity wire. The thermometer and the heater had been ground down to reduce their thickness and mass and hence their contribution to the specific-heat measurement. The addenda was less than 15% of the total specific heat. Figure 1(a) shows the experimental geometry with the sample sandwiched between the heater and the thermometer. The heat capacity C_p was measured using standard ac calorimetry techniques,¹¹ where sinusoidally time varying heat is supplied to the sample with the miniheater, and the amplitude of the ac temperature response (which is essentially inversely proportional to the heat capacity) is recorded as the magnetic field is swept.

For the measurement of C_p the low mass heater was driven with a 5.7 KHz current which was amplitude modulated by a low-frequency (between 1 and 1.8 Hz) sine wave, producing sinusoidal heating at twice the modulation frequency. The amplitude and phase response of the sinusoidal temperature excursion was checked with frequency sweeps at different temperatures to ensure that we were in the appropriate frequency region. The thermometer resistance was measured with a lockin amplifier at a frequency of 1.8 KHz. The output of this lockin (with a time constant of < 0.01 sec) was measured with another lockin referenced at the heat modulation frequency (2–3.6 Hz) to obtain the heat capacity. The dc temperature was measured by time averaging the output of the 1.8 KHz lockin over a few cycles of the temperature oscillation.

For magnetocaloric measurements the temperature evolution of the sample was monitored during field sweeps, with no external heat supplied to the miniheater. The heat evolved (absorbed) by the sample gives rise to a temperature rise (drop) of the sample. We may expect two distinct contributions. Latent heat from a first-order phase transition will appear as a sudden tempera-

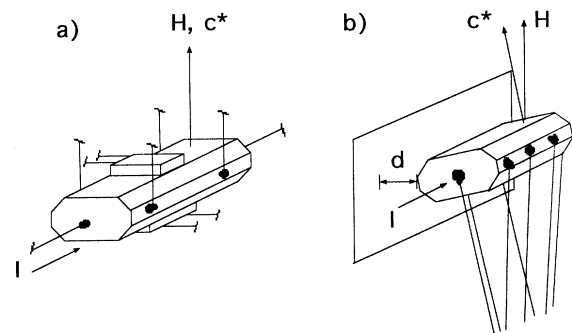


FIG. 1. Schematic of the experimental setups. (a) shows the calorimetric sample of $(\text{TMTSF})_2\text{ClO}_4$ sandwiched between a miniheater and a thermometer, and transport leads attached with silver paint. (b) shows the magnetization sample attached with silver paint at a distance d away from an electrode, and transport leads attached with silver paint.

ture change followed by an exponential relaxation to the probe temperature, where the relaxation time constant τ is given by $\tau = C_p/\kappa$. In the absence of a latent heat, the temperature excursion ΔT is a measure of $\partial S/\partial H$, where $\Delta T = T - T_0 \simeq [T_0(\partial S/\partial H)(dH/dt)]/K$ where (dH/dt) is the field sweep rate, and $(\partial S/\partial H)$ is the derivative of entropy with respect to field. The amplitude of the temperature changes is directly proportional to the sweep rate, whereas the latent heat contribution is independent of the sweep rate. Both of these contributions to the heat evolution reverse their sign when the field is swept down rather than up. The time constant C_p/κ varied with heat capacity, but it was always less than 1 s. Transport measurements were usually performed simultaneously with the thermodynamic measurements. ρ_{xx} and ρ_{xy} were measured with an ac 6 probe with a frequency of 137 Hz. ρ_{xy} measurements were performed by reversing the magnetic field and taking the odd component from the Hall leads as the Hall signal. For ρ_{xx} measurements were taken for both field orientations only once, at the lowest temperature, to verify that the ρ_{xy} component to the signal on this set of leads was less than 1%. Subsequent measurements were taken for one field orientation. Occasionally all the measurements, C_p , $\partial S/\partial H$, ρ_{xx} , and ρ_{xy} were performed separately to make sure that there was no interference. Fields were swept at rates between 40 and 100 G/sec.

The second sample was set up for the measurement of the anisotropic magnetization and ρ_{xy} of a 0.9 mg sample using a torque balance capacitance technique [Fig. 1(b)].¹² This sample was oriented such that c^* was at a small angle ($\simeq 12^\circ$) with the external field. It was suspended from 25 μm gold wires of length 7.5 mm. These wires were used to measure ρ_{xy} . In a homogeneous external field the sample will experience a torque $\tau = \mathbf{M} \times \mathbf{H}$, where \mathbf{M} is the anisotropic component of the magnetization. This torque causes the wires to bend until τ is balanced by the restoring torque of the transport wires from which the sample is suspended. The sample displacement is determined by measuring the change of the capacitance between the sample and an electrode nearby.¹² The torque balance is calibrated by applying a constant dc current through the sample and ramping the magnetic field. The Lorentz force on the sample displaces the sample towards or away from the electrode. The capacitance change due to this displacement is measured, and thus the relationship between capacitance and torque is obtained. The angle between c^* and the magnetic field was determined by matching one transition feature between samples 1 and 2. In addition we measured the resonant frequency of the torque balance and the sample mass, allowing a determination of the torque constant of the balance. With this information we determine the change of the angle between c^* and the field to be less than 1.2° for the maximal sample displacement in the measurement. We have measured magnetization and Hall effect in the same sample in fields up to 9 T, $T = 0.3$ K.

In a related set of experiments the same samples were cooled at a faster rate through the anion ordering transition to see the effect of anion disorder (sample 3) on

the magnetocaloric signal of $(\text{TMTSF})_2\text{ClO}_4$ at 0.5 K in fields up to 8 T. An additional experiment was performed on a sample (sample 4) mounted solely for transport studies in an effort to reduce the noise in the Hall measurement.

III. EXPERIMENTAL RESULTS

We will first present an overview of our results and then focus our attention on the details of the transitions. In Fig. 2 we show a compilation of data obtained with the first two experiments taken at $T \simeq 0.4$ K. The data for Figs. 2(a) and 2(b) were taken simultaneously, as was the data for Figs. 2(c) and 2(d). Data shown in 2(a)–2(d) are all from one sample. Traces for the magnetization sample are plotted against the H component along the c^* axis of this sample, and they are shown in traces 2(e) and 2(f). Traces where the field is swept up are plotted in solid lines, and down sweeps are plotted as dotted lines.

Evident in these data are the effects of the cascade of FISDW's. With increasing magnetic field the number of carriers is progressively reduced with each transition and, in general, the longitudinal resistance ρ_{xx} increases. The entropy and the specific heat are likewise progressively reduced and in the lower field transitions the specific-heat jumps associated with second-order transitions are clearly present. The Hall resistance increases as the carriers are reduced and the plateaus associated with the quantum Hall effect become more apparent at the higher field phases. The transitions between successive phases are also marked by jumps in the temperature proportional to $\partial S/\partial H$, and the magnetization increases (paramagnetically) on entering each new phase indicating the free-energy reduction. All of the transitions and transition features "line up" between all the measurements on a given sample, as the reader can verify by applying a ruler to the plots. As an illustration we have marked the positions of the two peaks observed in ΔT at about 5.2 T in curve 2(d) and the same fields are indicated in the other curves of the same sample [2(a)–2(d)]. We have also marked the equivalent field interval on traces 2(e) and 2(f) (sample 2) as matched by the ρ_{xy} trace. The positions mark slope changes in ρ_{xx} , ρ_{xy} , \mathbf{M} , and C_p suggesting the beginning and end of a transition region between two distinct phases. All of the other features in the ΔT curve can similarly be mapped to structures in the other curves. Another evident feature of the data is the large hysteresis present in the transitions around 7–8 T and the lack of hysteresis for the lower field data.

In Fig. 3 we show the phase diagram constructed from magnetic-field sweeps (as in Fig. 2) taken at different temperatures, as well as from a number of temperature sweeps at fixed fields. All the transition phase boundaries shown in this plot have been reproduced in other thermodynamic experiments on other samples. Before considering the phase boundary in detail we discuss some general aspects of the different measurements.

The low-temperature Hall resistance of samples 1 and 2 is depicted in Figs. 2(c) and 2(e), respectively. These traces are essentially identical, to within experimental

limits. They show the quantized Hall plateaus associated with the different FISDW phases with the last Hall plateau at $\rho_{xy} \simeq h/2e^2/\text{layer}$. (The values we obtain are $\rho_{xy} = 13.7 \text{ k}\Omega/\text{layer}$ for sample 1 and $\rho_{xy} = 13.8 \text{ k}\Omega/\text{layer}$ for sample 2 with an error of 5%. Note that $h/2e^2 = 12.906 \text{ k}\Omega$.) Both samples showed signs of cracking upon cooldown. The Hall signature of the transitions in both samples provide the yardstick for a correlation of the transition features observed in both samples. (In fact, we have used the Hall signature to determine and correct for the intentional misalignment of sample 2 with

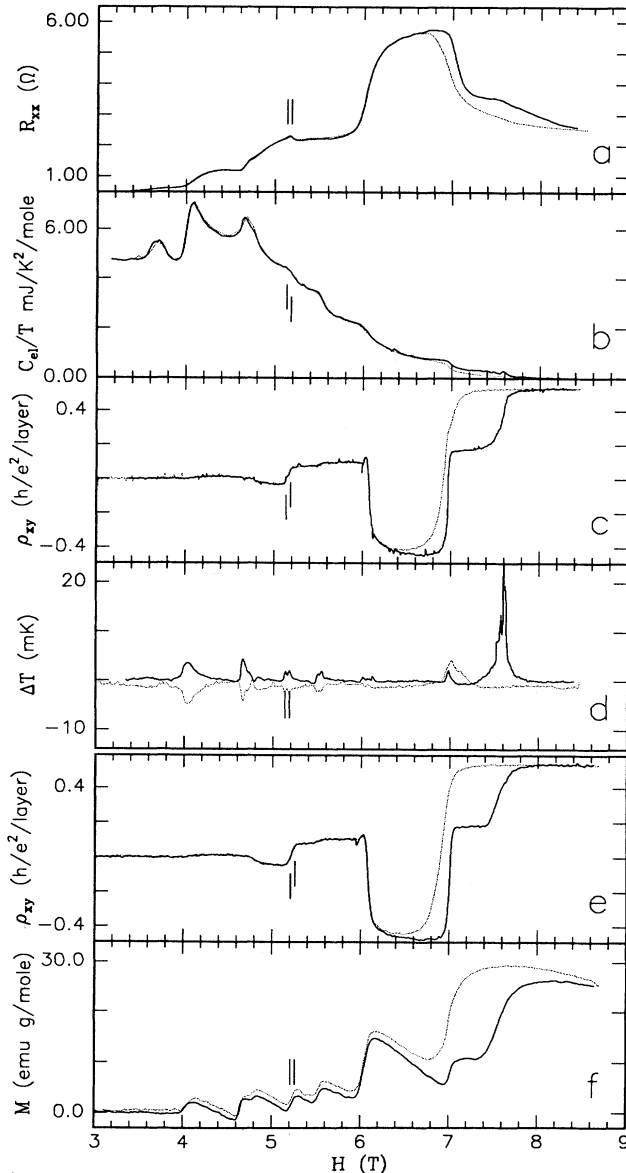


FIG. 2. Magnetic-field dependence of ρ_{xx} , C_{el} , ρ_{xy} , and ΔT (magnetocaloric effect) in $(\text{TMTSF})_2\text{ClO}_4$ (sample 1) at $T \simeq 0.35 \text{ K}$, shown in traces (a)–(d). Traces (a) and (b) are obtained simultaneously, as are traces (c) and (d). Magnetic-field dependence of ρ_{xy} and magnetization in $(\text{TMTSF})_2\text{ClO}_4$ (sample 2) at $T \simeq 0.32 \text{ K}$, shown in traces e and f.

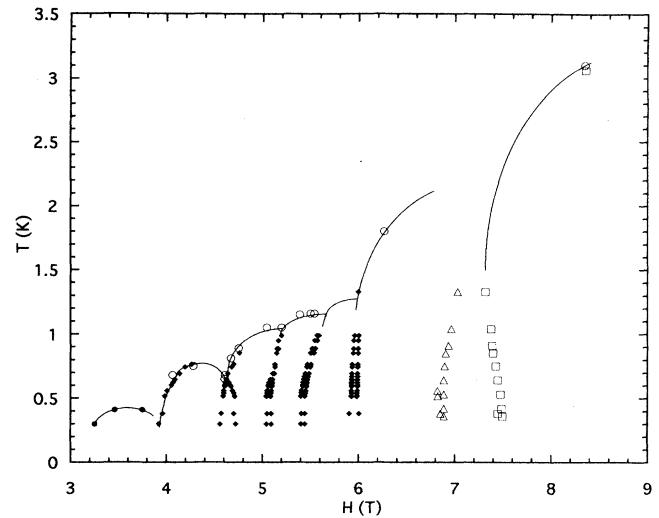


FIG. 3. Low-field phase diagram of $(\text{TMTSF})_2\text{ClO}_4$ compiled from data obtained in this series of experiments and Ref. 8. Lines are guides to the eye, solid diamonds magnetocaloric signals, circles from specific heat (solid circles are from field sweeps, hollow circles from temperature sweeps), squares and triangles from ρ_{xy} .

the applied field.) The presence of the well-developed Ribault Hall plateau⁴ between 6 and 7 T confirms that both samples are indeed well relaxed; the anions are ordered. Transitions between FISDW states are characterized by smooth changes of ρ_{xy} , with the exception of the transitions around the Ribault phase.

The magnetoresistance [Fig. 2(a)] shows a change of its slope from one transition to the next, with the exception of the transition seen at $H \simeq 5.5 \text{ T}$, where the magnetoresistance remains constant. As usual, the phase with the largest magnetoresistance is the Ribault phase. It may be significant that the magnetoresistance decreases at $H \simeq 5.2 \text{ T}$ and $H \simeq 7 \text{ T}$ for the two transitions with a change of the ρ_{xy} sign from negative to positive. The two regions of negative Hall sign have very similar shapes, already suggesting a family resemblance. In most previous magnetoresistance measurements, the stable high-field phase starting at 7.5 T is marked by a sharp increase in resistance to a value comparable to that of the resistance seen in the Ribault phase. Such behavior is reproducibly absent in the present work.

In the heat-capacity measurement [Fig. 2(b)] we confirm the discovery by Pesty and co-workers of a second metallic reentrance in between SDW phases at ($T = 0.4 \text{ K}$, $H = 3.9 \text{ T}$), where the heat capacity returns to the value of the metallic state observed at fields below the first FISDW transition.¹³ This reentrance feature is strikingly similar to the one associated with the “tetracritical point” at $T = 0.67 \text{ K}$, $H = 4.6 \text{ T}$ described in Refs. 8 and 14. At $H \simeq 3.6 \text{ T}$ we see the phase preceding the metallic reentrance as a smooth and small “bump,” whereas the one following the reentrance at 3.9 T shows a steep increase in C , though not a discontinuous one. Transitions are evident as slope changes $C(H)$ above $H \simeq 4.6 \text{ T}$, with C_{el} decreasing to 0 at $H \simeq 7.8 \text{ T}$. (Our value

of γ , the linear term in the heat capacity, differs from the results obtained by the Orsay group by a factor 2 at this temperature, while at higher temperatures between 1 and 2 K we measure $\gamma \simeq 10$ mJ/K²/mol, which is in agreement with their results. At this point we cannot rule out a systematic error causing this discrepancy.)

In the magnetocaloric measurement a question of interest is whether or not the phase diagram of (TMTSF)₂ClO₄ is indeed arborescent, that is consisting of many branches, since claims of such an arborescent phase diagram were based on magnetocaloric results by the Orsay group.⁵ We had previously found no such arborescence,⁸ and our present magnetocaloric results confirm our previous findings for yet a different sample with a slightly different cooling history, at temperatures as low as the ones attained in the original work finding arborescence. Field regions separating the clearly identifiable transition features, which we shall discuss below, show smooth behavior and some temperature noise, but no sign of new phases away from the transition regions.

In the anisotropic magnetization we see comparatively steep paramagnetic rises of the magnetization associated with the FISDW transitions, with subsequent decreases of magnetization as the sample goes deeper into the FISDW state associated with that field. Our value for the sample magnetization is a factor 3 smaller than the value quoted in Ref. 15. We attribute this discrepancy to the uncertainty associated with the angle between c^* and H , to which this technique is highly sensitive. Note a single zero crossing at ~ 4.5 T in the magnetization. This diamagnetic contribution indicates an energy increase and in the simplest models should coincide with a dip in the phase boundary.¹⁶ This is presumably associated with the reentrance at 0.7 K and 4.5 T.

IV. NATURE OF THE PHASE BOUNDARIES

We now turn our attention to the details of the transitions. In the standard model the transitions in between FISDW states are thought to be first order, for which one would expect to observe a discontinuous change of magnetization and entropy (latent heat) as the phase boundary is crossed. In our experiments we see two different regions of transitions. Below 6 T the transitions are reproducible and nonhysteretic. Above 6 T there is a marked hysteresis on field cycling and even for field sweeps in the same direction there are spikes and “noise” which differ from sweep to sweep. We first concentrate on the low-field region.

For $H < 6$ T the transitions between FISDW’s appear as transition regions of finite width. The lack of sharpness seen in most of the transitions arises intrinsically, and is not due to sample inhomogeneities, strain fields, etc. The sharpness in the peaks observed in $\Delta T \propto \partial S / \partial H$ show very narrow features. A primary example is the case of the two transition regions at $H \simeq 5.2$ T and at 5.55 T. The field region over which the magnetization changes from the minimum of one paramagnetic sawtooth to the maximum of the next coincides with the field interval over which the Hall resistance changes from

one plateau to the next [Figs. 2(e) and 2(f)]. These rises of the Hall resistance also coincide with the magnetocaloric double peaks characterizing these transition regions. The transition regions are about 0.1 T wide.

The FISDW’s are a type of Peierls instability of a metallic system where electronic energy is lowered by opening a gap at the Fermi energy. A distortion of the right periodicity to open such a gap costs less energy than the electronic energy gained. If a gap is already present, there is not much additional electronic energy lowering. Therefore the energy gain by making a distortion is maximum if there are no other gapping distortions present. This leads to a natural competition or repulsion between different FISDW phases.

We would therefore expect a repulsive term in the free energy when two SDW’s coexist. A phenomenological Landau expansion for a system with two competing order parameters, Φ_1 , Φ_2 , is

$$f = \frac{a_1}{2}(T - T_{c1})\Phi_1^2 + u_1\Phi_1^4 + \frac{a_2}{2}(T - T_{c2})\Phi_2^2 + u_2\Phi_2^4 + u_{12}\Phi_1^2\Phi_2^2. \quad (4.1)$$

In the absence of the last term this describes two non-interacting second-order phase transitions. We associate Φ_1, Φ_2 with neighboring FISDW phases having distinct quantum numbers and magnetic-field-dependent transition temperatures $T_{c1}(H)$, $T_{c2}(H)$. With $u_{12} = 0$ the phase boundary in the vicinity of the tetracritical point would look something like the schematic shown in Fig. 4(a). On entering the coexistence region from the low-field side Φ_1 is continuous and Φ_2 starts increasing from zero. On exiting the coexistence region Φ_2 is continuous and Φ_1 goes to zero. This is similar to the phase diagram expected from the standard model in the crossover regime between two SDW’s when their individual transition temperatures are calculated from the Stoner criteria using the normal-metal susceptibilities $\chi(\vec{q})$.²

The biquadratic form for the interaction term is the lowest coupling which does not act as an effective field from one order parameter to the other, i.e., it does not favor a particular correlation of the signs or phases of the order parameters. For repulsive interactions u_{12} is positive. If $u_{12}^2 < u_1u_2$ the phase boundary is simply modified by a smaller coexistence region as shown in Fig. 4(b). All transitions are still second order and there is a tetracritical point where the four phase boundaries connect. As u_{12}^2 increases the coexistence region narrows. When $u_{12}^2 > u_1u_2$ the two second-order lines about the coexistence region collapse into a single first-order line as shown in Fig. 4(c).

One of the most interesting aspects of the previous thermodynamic studies of (TMTSF)₂ClO₄ was the discovery of a tetracritical point^{5,14} in the phase diagram. Their finding corresponds to the data shown in Fig. 3 between 4.5 and 4.8 T. This observation led Lebed to examine the interaction between two SDW phases.⁶ His model takes into account the role of electron-electron Umklapp scattering (but omits the anion ordering effects) and yields a free energy of the form of Eq. (4.1) from a microscopic calculation. At first glance the tetra-

critical point is in agreement with the Landau expansion of Eq. (4.1), and the splittings in the phase boundaries at higher field are not. However, if the repulsion of different SDW phases is temperature dependent such that

$$u_{12}^2 > u_1 u_2 \rightarrow u_{12}^2 < u_1 u_2 \text{ as } T > T_b \rightarrow T < T_b, \quad (4.2)$$

then above T_b there is a first-order transition line which splits at T_b to two second-order lines as schematized in Fig. 4(d). So we see that a simple Landau model can generate the observed phase boundaries. But we also need to ask how these different scenarios for going from one SDW phase to another will affect the transport properties and the magnetization. On the one hand, for a single first-order transition we should simply have a discontinuous change in all of the properties (and a latent heat in the magnetocaloric effect) and probably some sign of hysteresis. This is not observed in the low-temperature data below 6 T. If on the other hand there are two second-order transitions and therefore a coexistence region, we would expect a gradual change from the behavior in one phase to that in the next. This is indeed what we see at

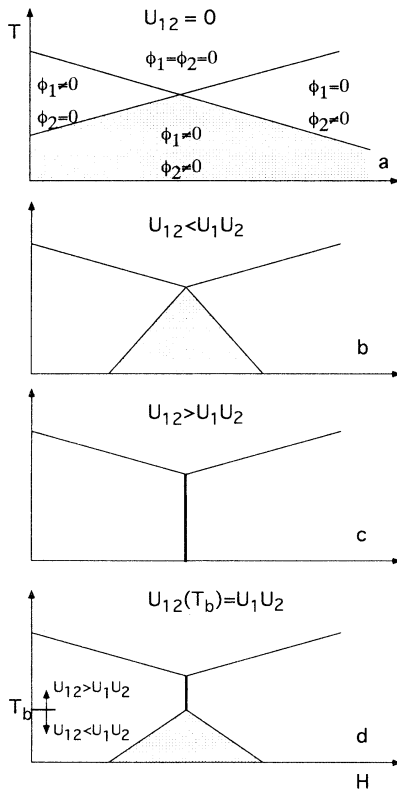


FIG. 4. Schematic phase diagrams arising from the simple Landau model described in Eq. (4.1). Fat lines correspond to first-order transitions, thin lines to second-order transitions. In (a) there is no interaction between phases. In (b) there is a small repulsion between phases which reduces the coexistence region. In (c) the repulsion is strong enough to prevent coexistence and the result is a first-order transition. For a temperature-dependent repulsion we can have the splitting shown in (d).

the transitions at 5.1 and 5.4 T in magnetization, specific heat, ρ_{xx} , and ρ_{xy} . The entrance and exit of the coexistence region appear to be marked by peaks in $\partial S/\partial H$.

Special attention should be paid to the behavior of the Hall effect. Machida and co-workers⁷ have shown that with two coexisting SDW order parameters the ρ_{xy} should abruptly change from one quantized value to the next somewhere in the middle of the coexistence phase as the amplitudes of the two order parameters change and the topological winding number jumps. We see a much more gradual change. However, exactly when the winding number jumps there must be a vanishing of the gap somewhere on the Fermi surface. At this point there is no longer a quantized Hall effect. At finite temperatures we might expect that excitations over the small gap on part of the Fermi surface allows for unquantized ρ_{xy} values and a gradual transition of ρ_{xy} across the entire coexistence region.¹⁷ We therefore suspect that the 5.1 and 5.4 T (as well as the 5.9 T) transitions are well described by the scenario of Fig. 4(d) and the underlying Eq. (4.1).

What then of the original tetracritical point at 4.6–4.8 T? Does it correspond to Fig. 4(b)? Unfortunately not. As investigated in detail in Fig. 5, there is a new Hall plateau that is well defined between the phase boundaries. The signatures of this region are a jump in magnetocaloric signal on entering the new phase at 4.6 T and a magnetocaloric signal in the opposite direction on leaving at 4.8 T. Moreover, associated with each $\partial S/\partial H$ feature is a jump in magnetization. The magnetic Clausius-

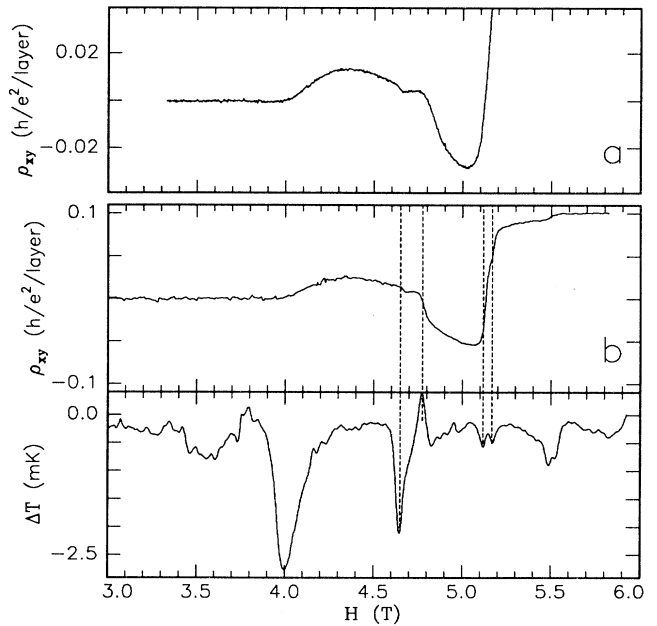


FIG. 5. Magnetic-field dependence of ρ_{xy} in $(\text{TMTSF})_2\text{ClO}_4$ (sample 4) at $T \simeq 0.4$ K, shown in trace (a). A new Hall plateau is visible at $H = 4.54$ T. Magnetic-field dependence of ρ_{xy} and ΔT (magnetocaloric effect) in $(\text{TMTSF})_2\text{ClO}_4$ (sample 1) at $T \simeq 0.35$ K, shown in traces (b) and (c), which were obtained simultaneously. The new Hall plateau coincides with the phase emerging from the multicritical point at ~ 4.7 T.

Clapeyron equation relates the change in entropy and the change in magnetization across a first-order phase transition to the slope of the phase boundary. While it is not possible from the present data to separate the latent-heat contribution to the temperature excursions from the continuous change of $\partial S/\partial H$, we would like to point out that the signs of the magnetocaloric features and the magnetization jumps are consistent with a Clausius-Clapeyron interpretation of the transitions. Entropy and magnetization increase at the 4.6 T transition and $\partial T_{\text{SDW}}/\partial H$ is positive and magnetization increases, entropy decreases and $\partial T_{\text{SDW}}/\partial H$ is negative at 4.8 T. We associate this “tetracritical” point as rather the intersection of two second-order lines (the boundary with the metallic phase at high temperature) with two first-order lines. The sign reversal of $\partial S/\partial H$ then results from the Clausius-Clapeyron equation and the sign reversal for the phase boundaries at 4.6 and 4.8 T. The microscopic explanation for this behavior awaits theoretical treatment.

We now consider the transitions above ~ 6 T. The transition upon entering the Ribault anomaly at $H \simeq 6$ T is characterized by a double peak in the magnetocaloric signal, as for the lower field transitions, though this signal is washed out when the field is swept down. The peak separation is slightly larger than that of the preceding double peaks. As before the magnetization rises continuously over the field region defined by those two peaks. At the lowest temperatures the Hall resistance rises a small amount and then changes sign and drops to $\simeq 80\%$ of the ρ_{xy} value at the center of the Ribault anomaly in the same field interval. The heat release at this transition is less than that for the double peaks discussed above, whereas the sharp rise in magnetization associated with this transition region is considerably larger than the two preceding it.

At $H \simeq 7$ T we find the next transition which, unlike the three transitions discussed above, is characterized by a single magnetocaloric peak. This peak is about 0.1 T wide, and it coincides with a sharp rise and sign change of the Hall resistance as well as with a rise of magnetization. The FISDW phase following this transition is highly hysteretic; it is only observed when the field is swept up, and it is skipped when the field is swept back down.

At $H \simeq 7.5$ T we find the last low-field transition to a very stable high-field phase (which persists to $H \geq 23$ T), characterized by a very large irreversible heat release, a large change of magnetization and a broad rise of the Hall resistance to a saturated value of about $h/2e^2/\text{layer}$; these changes occur over a field range of about $\simeq 0.3$ T. Upon sweeping the field back, down the phase between 7.5 and 8 T is skipped and the transition is from the stable high-field phase to the Ribault phase; again there is considerable irreversible heat release.

The main distinguishing character of this field region is the irreversible heat release accompanying the transitions for both up and down field sweeps. The heat release stops when the field ramp is stopped in this field region, and it resumes when the field sweep resumes in the same direction, even after sitting in a static field for about a

minute. We associate this “quaky,” irreversible behavior with pinning and dissipative motion of domain walls spatially separating the different SDW phases in a series of very strongly first-order phase transitions. Such strong pinning may result from coupling of the SDW order parameter to the lattice. The magnetocaloric measurement for the 6.9 and 7.5 T transitions show a series of sharp quaky heat releases on increasing the field. At first glance one might attribute this behavior to the latent heat of a first-order transition which “gets stuck” on lattice defects or other pinning sites. However, a similar *heat release* is observed on lowering the field. This cannot result from inherently reversible latent heat. In the present case the jerky motion of the domain walls must lead to “friction” and/or viscous dissipation. The difference in integrated heat release between a field upsweep and downsweep shows that there is a latent heat that is comparable to, but less than the irreversible loss.

We now describe the effect of anion ordering on the magnetocaloric signature of the transitions. We show in Fig. 6 the magnetocaloric data for the same sample at the same base temperature and field sweep rate, the only difference being the degree of anion ordering. Trace 6(b) was discussed in Ref. 8, and it shows the all the features discussed for sample 1 above. For the faster cooling rate (≥ 0.1 K/min) we now see the following changes of the magnetocaloric signal: The signature of the narrow phase below what before was a tetracritical point vanishes altogether, as does the double peak at 5 T. In its place there is a transition that is as broad as the double peak feature in the slow-cooled sample. The transition occurs at a lower field for the less relaxed sample, a shift of about 0.1 T. The next double-peak transition at $H \simeq 5.4$ T is still clearly visible in the more disordered sample, and it is shifted to a slightly lower field as well. This double-peak feature, which seems comparatively impervious to the effects of anion disorder, also persists to higher temperatures than the one which precedes it in a relaxed sample.

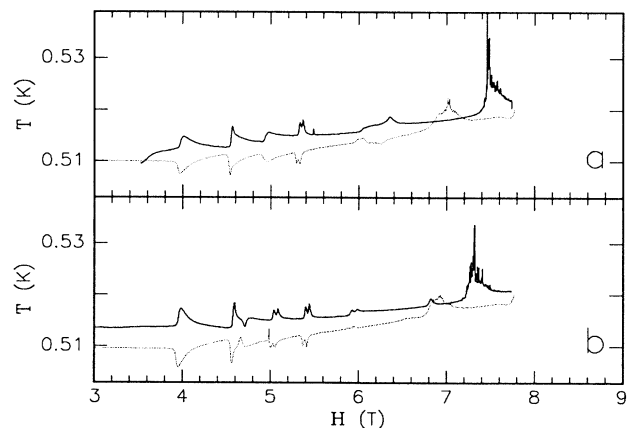


FIG. 6. Magnetocaloric effect for fast-cooled sample (a) and slow cooled sample (b). Note the vanishing of most of the double peaks and the reduction of the “Ribault” phase which is from 5.9 to 6.8 T in the slow-cooled sample and from 6 to 6.4 T in the fast-cooled sample.

As in the well ordered sample the magnetocaloric signal above 6 T is characterized by very large hysteretic and irreversible entropy flow, i.e., exothermic behavior for both upsweeps and down sweeps. When comparing the traces in Fig. 3 it appears that the anion disorder gives rise to an increased asymmetry between up and down sweeps. A small exothermic peak which marks the transition from the Ribault phase to the next FISDW state is visible in the upsweeps of both the relaxed (6.8 T) and the less relaxed sample (at 6.4 T). The field at which this transition occurs is markedly shifted to a lower value as anion disorder increased. This is consistent with the well established dependence of the Ribault anomaly on anion order, where anion disorder reduces the Ribault phase.

A. Temperature dependence of the Hall resistance

For $T=0$ different values of ρ_{xy}/layer have been predicted. The Hall index defined by $n = h/2e^2/\rho_{xy}$ has been predicted to take on various successive values such as $n = (1, 3, 5, \dots)$.¹⁰ (In this model by Osada, Kagoshima, and Miura the anion order potential is responsible for the suppression of even integer Hall plateaus, and for the metallic reentrance at fields above $\simeq 14$ T.) Alternatively, ratios of ρ_{xy} values (1/3, 1, Ribault, 2, 3, ...) have been observed/suggested. In the present study the highly stable phase above 9 T saturates to a ρ_{xy} value of n nearly 1.¹⁸ Most of the lower field phases, however, appear not to have attained their saturation value of ρ_{xy} at temperatures of $T = 0.3$ K, as we show in Fig. 7. We plot the values of the ρ_{xy}/layer for several phases, divided by the value of $\rho_{xy}(9 \text{ T})$, which has saturated to $\rho_{xy} \simeq 0.5h/e^2$. (We normalize to eliminate the $\simeq 5\%$ uncertainty arising from the measurement of the thickness of the sample.) While it is not possible based on our data to determine the saturation values, we can compare the ρ_{xy} plateau sequences mentioned above: At $T = 0.3$ K the sequence we observe is $n \simeq (1, 3, \text{Ribault}, 5, 12, 5, 9, \dots)$. If we ignore for the moment the Ribault anomaly, which has not attained a saturated value at $T = 0.3$ K, then it appears that at least the ratio sequence (1, 3, 5) predicted by Osada for the positive hall values is plausible; however, at higher fields recent experiments suggest a picture in which anion order plays an important role and which is more complex than Osada's model.¹⁹

B. Higher temperature C vs H

We have also measured simultaneously the heat capacity and resistance at $T = 1.5$ K, where fast oscillations periodic in $1/H$ appear in resistance.⁹ We find no such oscillations in heat capacity, to within 10% of the electronic heat capacity, which suggests that these oscillations are not of thermodynamic origin. This distinguishes the low-field behavior of $(\text{TMTSF})_2\text{ClO}_4$ from the high-field be-

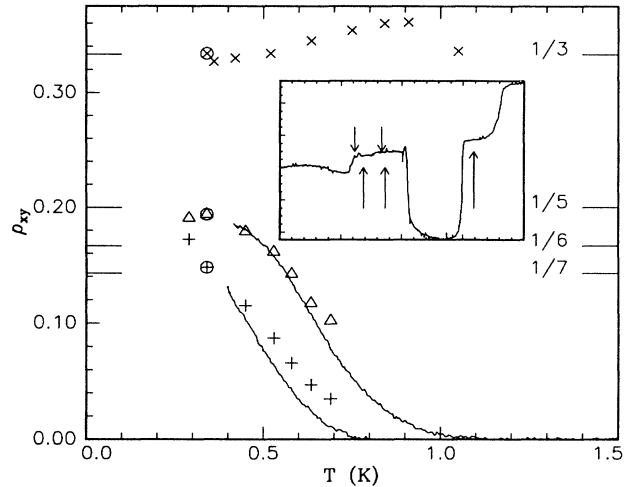


FIG. 7. Temperature dependence of $\rho_{xy}(H)/\rho_{xy}(9 \text{ T})$. Sample 1: $\triangle H = 5.37 \text{ T}$; $+$ $H = 5.75 \text{ T}$; $\times H = 7.18 \text{ T}$. Solid lines show temperature sweeps at $H = 5.23 \text{ T}$ and $H = 5.67 \text{ T}$, fields corresponding to the same Hall plateaus as \triangle and $+$, respectively. The discrepancy towards higher temperatures arises from the roundness of the Hall plateaus. Sample 2: circled symbols.

havior above $H \simeq 17 \text{ T}$, where these fast oscillations are observed both in magnetization and heat capacity.^{15,20}

V. CONCLUSION

The main finding of this paper is that throughout the complex phase diagram of $(\text{TMTSF})_2\text{ClO}_4$ there is complete coincidence of the thermodynamic and transport measured transitions. This relationship, particularly between the FISDW transitions and the quantum Hall steps, had been brought into question in a number of theoretical papers. We find that the different FISDW phases interact repulsively and that this leads either to a first-order transition or to a narrow coexistence region bounded by a set of second-order transitions. Both behaviors are observed in the phase diagram. We find no evidence for an “arborescent” phase diagram. The previously reported tetracritical point in the phase diagram appears instead to be the joining of two first- and two second-order lines and introduces an unheralded phase with a distinct Hall plateau. As side matters we also find support for the absence of “even” integer QHE phases, and for strong pinning and losses in the strongly first-order phase transitions.

ACKNOWLEDGMENTS

We would like to acknowledge discussions with Dr. Lebed, Dr. Machida, and Dr. Pesty and substantial conversations with Dr. Yakovenko. Research supported by NSF DMR92-16155.

- ¹ For a review, see T. Ishiguro and K. Yamaji, *Organic Superconductors* (Springer-Verlag, Berlin, 1990), for more recent references see, G. Danner, W. Kang, and P. M. Chaikin, *Physica B* **201**, 442 (1994); G. M. Danner *et al.*, *Synth. Met.* **70**, 731 (1995).
- ² L. P. Gor'kov and A. G. Lebed, *J. Phys. (Paris) Lett.* **45**, L433 (1984), P. M. Chaikin, *Phys. Rev. B* **31**, 4770 (1985); G. Montambaux, M. Heritier, and P. Lederer, *J. Phys. (Paris) Lett.* **45**, L533 (1984); M. Heritier, G. Montambaux, and P. Lederer; *ibid.* **45**, L943 (1984); K. Yamaji, *J. Phys. Soc. Jpn.* **54**, 1034 (1985); M. Ya Azbel, Per Bak, and P. M. Chaikin, *Phys. Lett. A* **117**, 92 (1986); K. Maki, *Phys. Rev. B* **33**, 4826 (1986).
- ³ W. Kang, S. T. Hannahs, and P. M. Chaikin, *Phys. Rev. Lett.* **70**, 3091 (1993).
- ⁴ M. Ribault, *Mol. Cryst. Liq. Cryst.* **119**, 91 (1985).
- ⁵ F. Pesty and P. Garoche, *Fizika (Zagreb)* **21**, 40 (1989); F. Pesty, P. Garoche, and M. Heritier, in *The Physics and Chemistry of Organic Conductors*, edited by G. Saito and S. Kagoshima, Springer Proceedings in Physics, Vol. 51, (Springer, Berlin, 1990); G. Faini, F. Pesty, and P. Garoche, *J. Phys. (Paris) Colloq.* **49**, C8-807 (1988).
- ⁶ A. Lebed, *JETP Lett.* **51**, 663 (1990).
- ⁷ K. Machida, Y. Hori, and M. Nakano, *Phys. Rev. Lett.* **70**, 61 (1993); K. Machida *et al.*, *Phys. Rev. B* **50**, 921 (1994).
- ⁸ U. Scheven, W. Kang, and P. Chaikin, *J. Phys. IV (Paris) Colloq.* **C2**, 287 (1993) [Suppl. to *J. Phys. I* **3** (1993)].
- ⁹ P. M. Chaikin *et al.*, *Phys. Rev. Lett.* **51**, 2333 (1983); H. Schwenk, *et al.*, *ibid.* **56**, 667 (1986); T. Osada *et al.*, *Solid State Commun.* **60**, 441 (1986); *Physica* **143B**, 403 (1986); J. P. Ulmet *et al.*, *ibid.* **143B**, 400 (1986); X. Yan *et al.*, *Phys. Rev. B* **36**, 1799 (1987).
- ¹⁰ K. Osada, S. Kagoshima, and N. Miura, *Phys. Rev. Lett.* **69**, 1117 (1992).
- ¹¹ P. F. Sullivan and G. Seidel, *Phys. Rev.* **173**, 679 (1968).
- ¹² J. S. Brooks, M. J. Naughton, R. V. Chamberlin, and P. M. Chaikin, *Rev. Sci. Instrum.* **58**, 117 (1987).
- ¹³ F. Pesty, P. Garoche, and K. Bechgaard, *Phys. Rev. Lett.* **55**, 2495 (1985).
- ¹⁴ F. Tsobnang, F. Pesty, P. Garoche, and M. Heritier, *Synth. Met.* **41-43**, 1707 (1991).
- ¹⁵ M. J. Naughton, J. S. Brooks, L. Y. Chiang, R. V. Chamberlin, and P. M. Chaikin, *Phys. Rev. Lett.* **55**, 969 (1985).
- ¹⁶ G. Montambaux *et al.*, *Phys. Rev. B* **39**, 885 (1989).
- ¹⁷ Victor Yakovenko (private communication).
- ¹⁸ W. Kang and D. Jerome, *J. Phys. (France) I* **1**, 449 (1991).
- ¹⁹ S. K. McKernan, S. T. Hannahs, U. M. Scheven, G. M. Danner, and P. M. Chaikin, *Phys. Rev. Lett.* (to be published).
- ²⁰ N. A. Fortune *et al.*, *Phys. Rev. Lett.* **64**, 2054 (1990); J. S. Brooks *et al.*, in *Advanced Organic Solid State Materials*, edited by L. Y. Chiang, P. Chaikin, and D. I. Cowan, MRS Symposia Proceedings No. 173 (Materials Research Society, Pittsburgh, 1990), p. 217.